COMPACT NEAR-NAVIGATION-GRADE IFOG INERTIAL MEASUREMENT UNIT IMU400

Yu.N. Korkishko[1,2], V.A. Fedorov[1,2], S.V. Prilutskiy[1,2], D.V. Obuhovich[1,2], I.V. Fedorov[1,2], V.E. Prilutskiy[1,2], V.G. Ponomarev[1], A.I. Zuev[1,2], V.K. Varnakov[1,2], I.V. Morev[1,2], S.M. Kostritskii[1,2]

[1] LLC RPC Optolink
Sosnovaya alley, building 6a, premises 5
124489, Zelenograd, Moscow
RUSSIA

[2] SIA Fiber Optical Solution
Podraga street 2a
LV-1007, Riga
Latvia

Inertial Sensors and Systems 2020
Braunschweig, Germany

978-1-7281-6848-7/20/$31.00©2020 IEEE

Abstract

At present time interferometric fiber-optic gyroscopes (IFOG, FOG) are widely used in inertial navigation systems (INS), and in wide range of applications have replaced its well-established main competitor ring laser gyroscopes (RLG). Recently, in order to cover the mass-market applications spectrum requiring low-cost and compact inertial sensor yet as much precise as it can be, RPC Optolink has launched new IFOG-based product: ultra-compact navigation-grade inertial measurement unit IMU400, its SWaP properties are: 80×95×62 mm, 0.7 kg, 0.5 l, ≤7 W. The aim of the current work was the production of IMU400 devices batches first, and then estimation of IMU 2019-2020 batches performance with direct approach and also with strapdown inertial navigation system (SINS) simulation methods, which is indirect way of performance observation, by its sense. Main IMU400 Gyro (FOG) and Accelerometer (ACC) parameters are: Angle Random Walk (ARW) = 0.007 °/√hour, Bias Instability (BI) = 0.01°/h; Velocity Random Walk (VRW) = 40μg/√Hz, BI = 6μg. SINS performance (best): heading 0.2°×sec(lat) (1σ, 10 min alignment time).

1. Introduction

At present time interferometric fiber-optic gyroscopes (IFOGs) are widely used in inertial navigation systems (INS), and in wide range of applications have replaced its well-established main competitor ring laser gyroscopes (RLG). In high precision closed-loop configuration of IFOG the feedback mechanism keeps the zero signal level by compensating the Sagnac phase shift with additional phase counter-shift. The value of the phase counter-shift allows one to obtain information about the angular rate of the device rotation [1-3].

Today the interferometric fiber-optic gyroscopes reach ultimate theoretical performance that allows to surpass RLG [2]. Due to its inherent low noise and its scalability, FOG technology is one of the very few technologies able to cope with the applications requiring the highest performance combined with cost and SWaP.

2. IMU400 design

Research & Production Company Optolink and its subsidiary company “Fiber Optical Solution” (Latvia) have so far developed [3] and produce series of single-axis FOGs SRS5000 [4], SRS2000, SRS1000 [5], SRS501 and SRS200 with different fiber coil lengths and diameters, as well as three-axis FOGs TRS500 and inertial measurement units (IMU) IMU400C, IMU500, IMU501, IMU1000, and IMU5000 [6], based on three FOG

channels and three precise quartz pendulous accelerometers. Space grade gyroscopes VOBIS are also produced and operate successfully on satellites at GEO [7].

Recently, in order to cover the mass-market applications spectrum requiring low-cost and compact inertial sensor yet as much precise as it can be, Optolink has launched new product: ultra-compact navigation-grade inertial measurement unit IMU400. External and internal view (gyro coils) of IMU400 is shown in Figure 1. The aim of the current work was the production of pilot IMU400 devices batch and the estimation of the performance of IMU with direct approach and also with strapdown inertial navigation systems (SINS) simulation methods, which by sense is indirect way of performance observation. To date, more than 100 units have been delivered to customers.

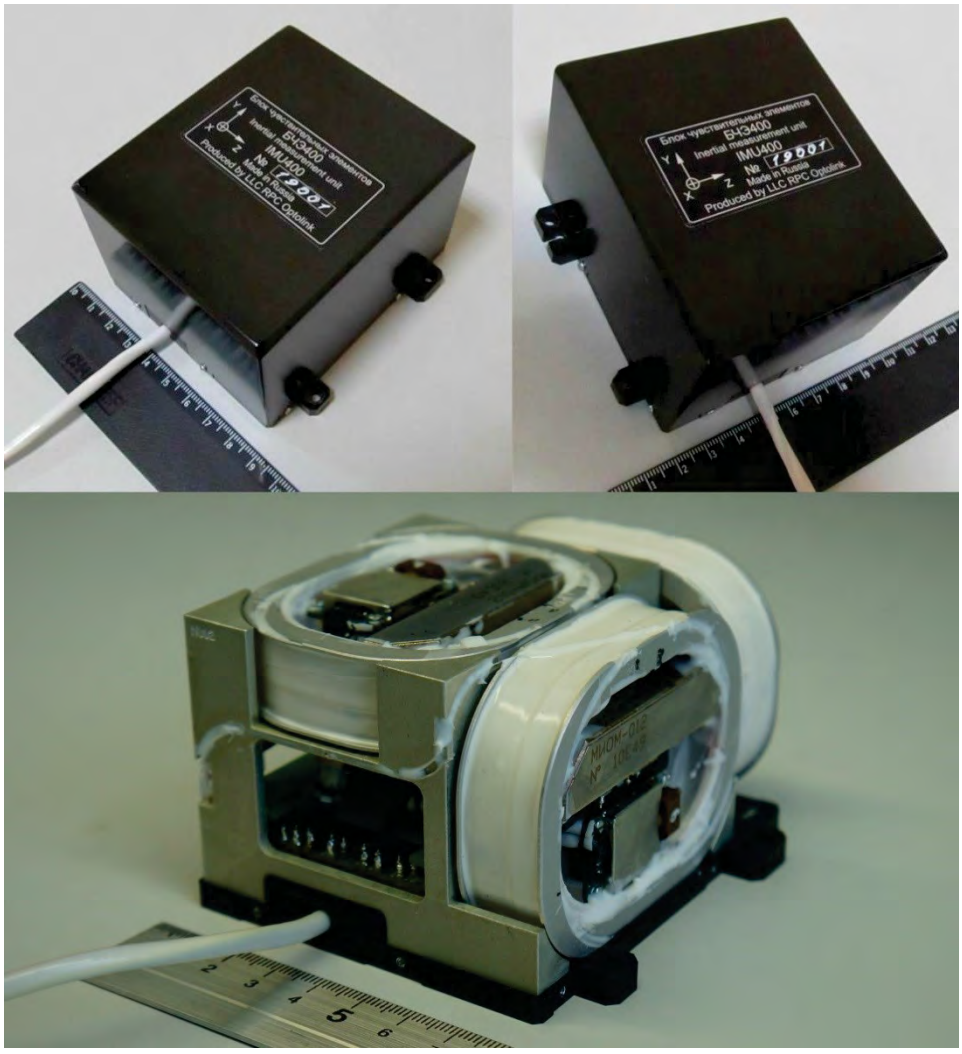

Figure 1. Image of IMU400

IMU400 SWaP properties are: 80×95×62 mm, 0.7 kg, 0.5 l, ≤7 W. FOGs are fed with single light source, coils are designed in the shape of rectangle with rounded corners.

In future, additional versions of circular fiber coils may appear, with slightly increased (worse) ARW but with less (better) temperature instability (down to 0.1°/hour, 1σ, in temperature range).

To cut down the size and cost, regularly used in all Optolink's other IMUs quartz pendulous accelerometers were substituted by MEMS. Each IMU400 has 3 triads (physical) of MEMS accelerometers, with 6 low-noise (composing 2 effective triads) and 3 high-noise acceleration channels which are neglected. Acceleration value along each axis is composed of 2 low-noise signals from different physical triads. While the temperature compensation of scale factors, biases and non-linearities is performed as whole, in order to achieve better accuracies misalignment temperature corrections are performed standalone for each of 2 effective triads before mixing. Also, the combination of 2 signals in each channel enables us to mutually mitigate bias and scale factor instabilities and temperature dependences, while effective accelerometer (size effect) lever arms do not exceed 10 mm, with an absolute average of <5mm.

Spatial displacement of 3 physical MEMS-accelerometer triads inside the IMU400 is presented in Fig. 2. IMU effective center, which is defined by accelerometric lever arms minima, coincides with the IMU physical center with maximum shift of 1.5mm.

IMU400 has both top and bottom magnetic shield.

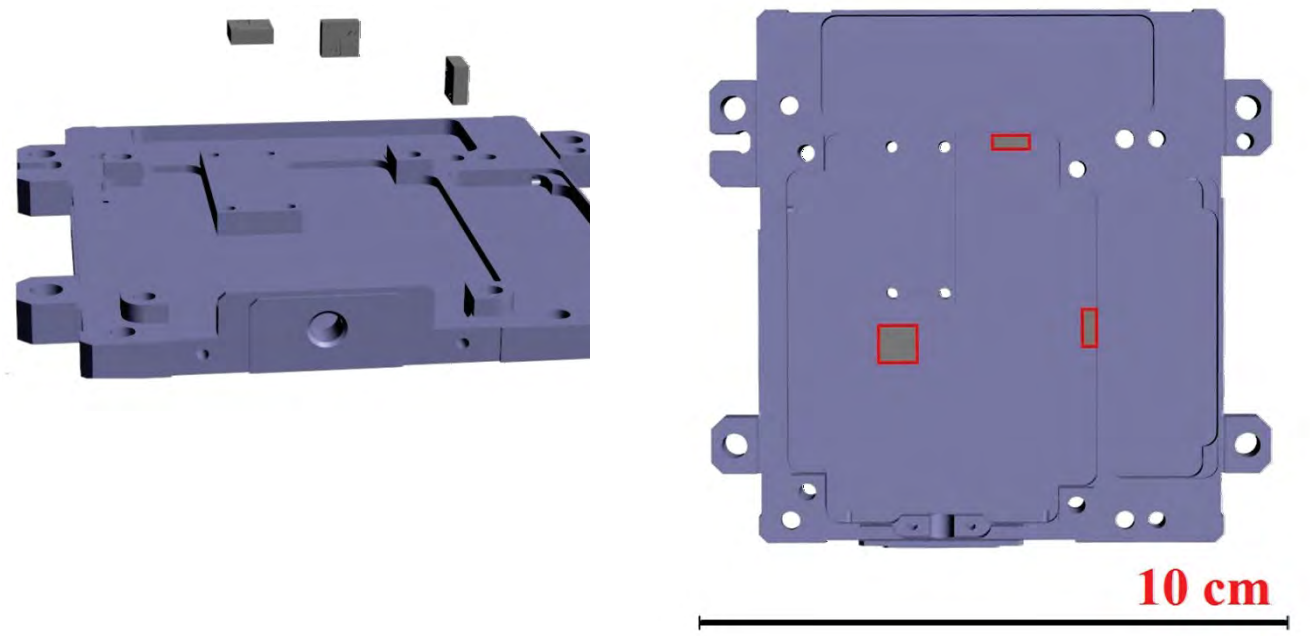

Figure 2. Spatial displacement of 3 physical MEMS-accelerometer triads inside the IMU400. Scale bar is applicable only for the right drawing.

3. IMU400 characterictics and properties

Specification for IMU400 with respect to IMU500 device is shown in Table 1. By * additional precise calibration values are specified. Maximum angular rate range can be decreased by factory tuning in order to comply with export or end user restrictions.

Table 1. Specification for IMU400 and IMU500

Performance	IMU400	IMU500
Gyro		
Angular rate range, °/s	±550 (max)	±400
Bias drift at constant temperature (1σ, 100s-averaging), °/h	0.1	0.1
Bias drift (1σ, 100s-averaging) in operational temperature range, °/h	0.7 (*0.3)	0.5 (*0.1)
Angle random walk, °/ √h	0.01	0.007
Scale factor error, ppm	500 (*200)	500 (*100)
Bandwidth, Hz	up to 1000 (user defined)	
Accelerometers		
Range, g	±10	±10 (**±50)
Bias drift at constant temperature, mg	1	0.5
Bias drift in operational temperature range, mg	1.0 (*0.4)	1.0 (*0.15)
Scale factor error, ppm	500 (*300)	500 (*100)
Noise power density, mg/ √Hz	0.08	0.05
Bandwidth, Hz	up to 300 (user defined)	
Physical Characteristics		
Misalignment, °	0.08 (*0.015)	
Output sample rate, Hz	up to 2000 (user defined)	
Power supply, V / Consumption, W	5 / 7	5, 24~36 / 10
Digital output interface	RS-422	RS-422 / 485
Operational temperature range, °C	-40 ~ +60	-40 ~ +60
Dimensions, mm	80 × 95 × 62	110×110×90
Weight, kg	0.7	1.4

Root Allan variance (deviation) curves of IMU400 FOGs (Fig.3) and ACCs (Fig.5) are presented: FOG - ARW 0.005-0.007 °/√h, bias instability <0.01 °/h, run-to-run 0.015 °/h, scale factor error 100 ppm; ACC - VRW 40 µg/√Hz, bias instability 6 µg, run-to-run 20 µg, scale factor error 150 ppm.

IMU400 gyroscopes Allan variance plot in Optolink's FOG family is presented in Fig. 4.

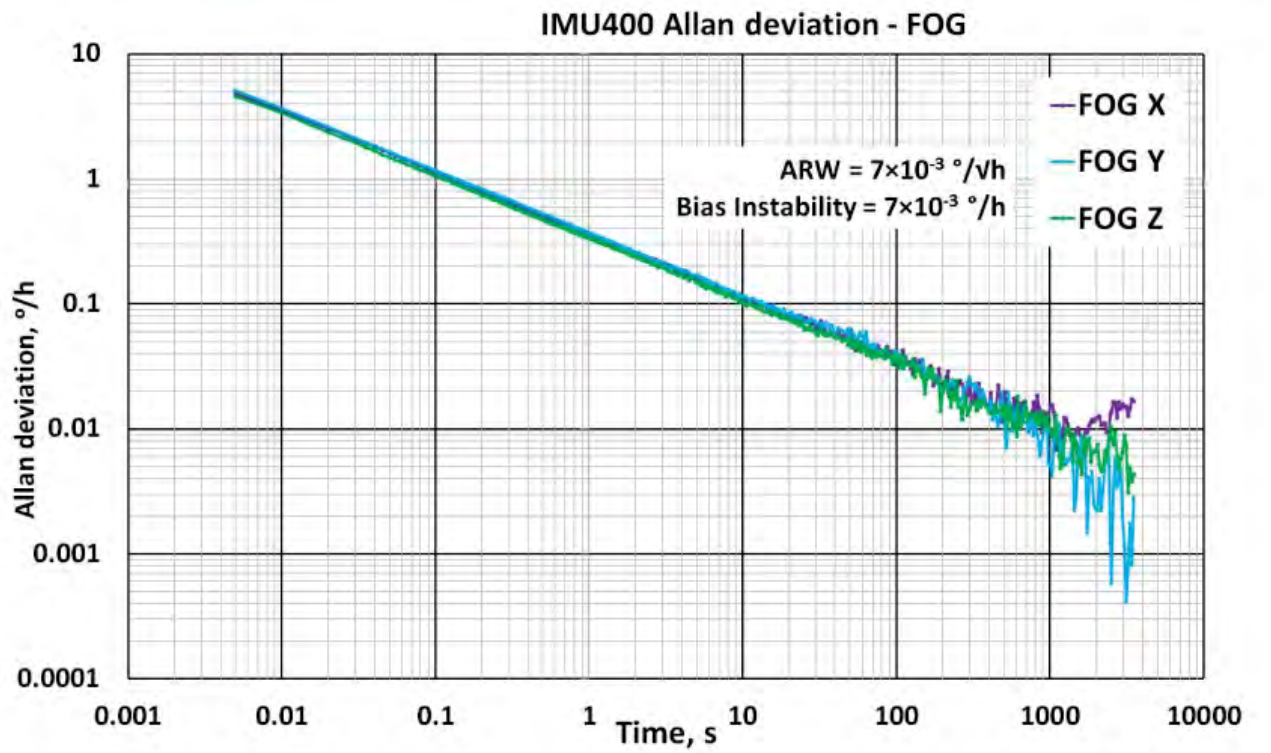

Figure 3. IMU400 Gyroscopes root Allan variance (deviation) plot

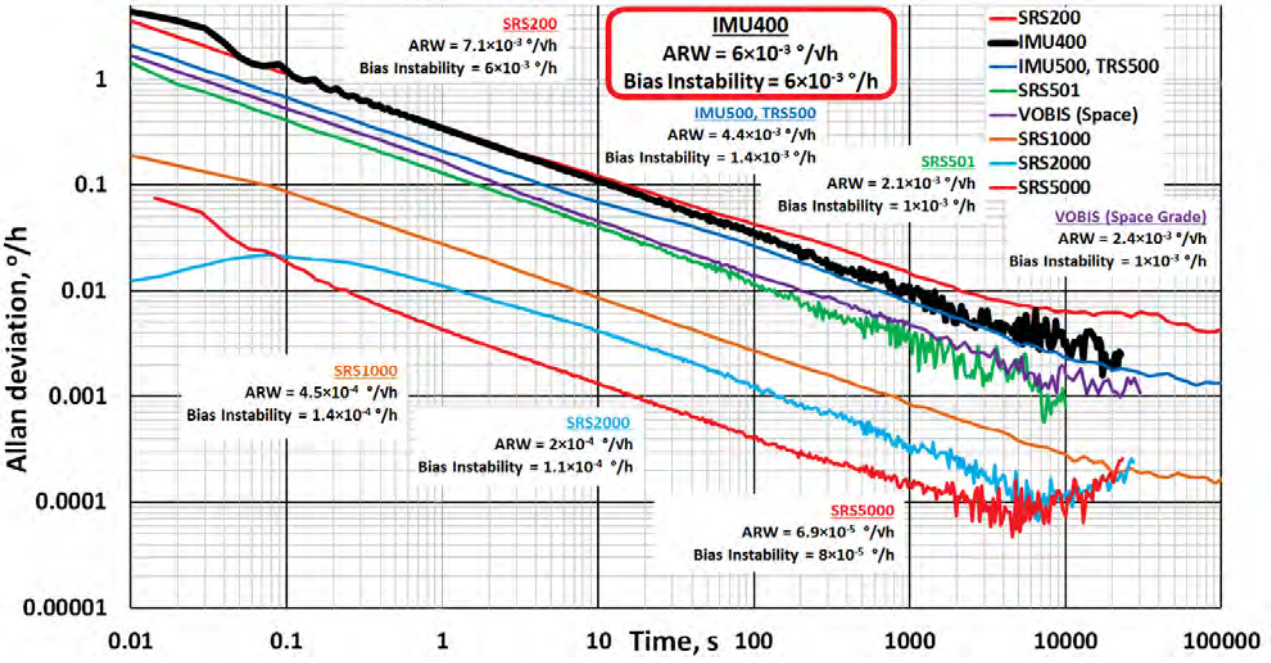

Figure 4. IMU400 gyroscopes Allan Variance plot in Optolink's FOG family

All obtained performance values are equivalent for each device channel.

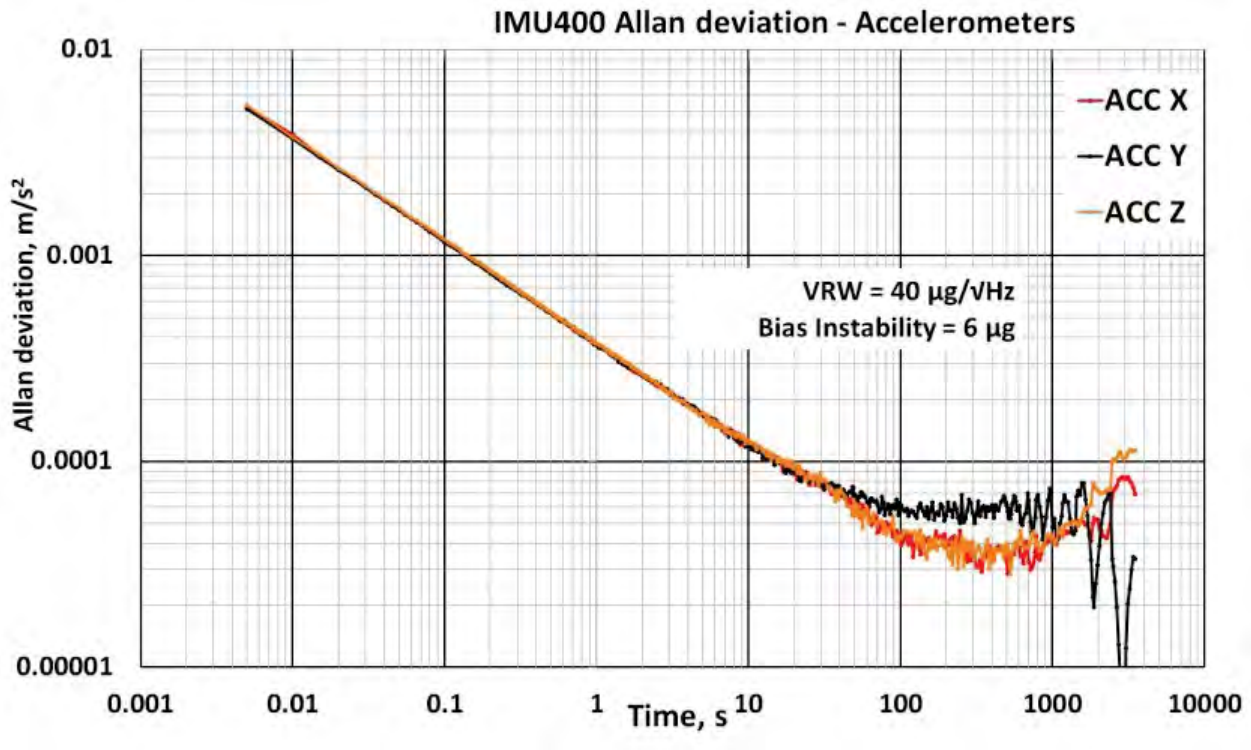

Figure 5. IMU400 Accelerometers root Allan variance (deviation) plot

In temperature range IMU400 units also shows stable behavior (shown in Fig. 6, Fig. 7), with gyro and ACC bias drift (100s-averaging RMS, 1σ) of <0.1°/hour and <100µg.

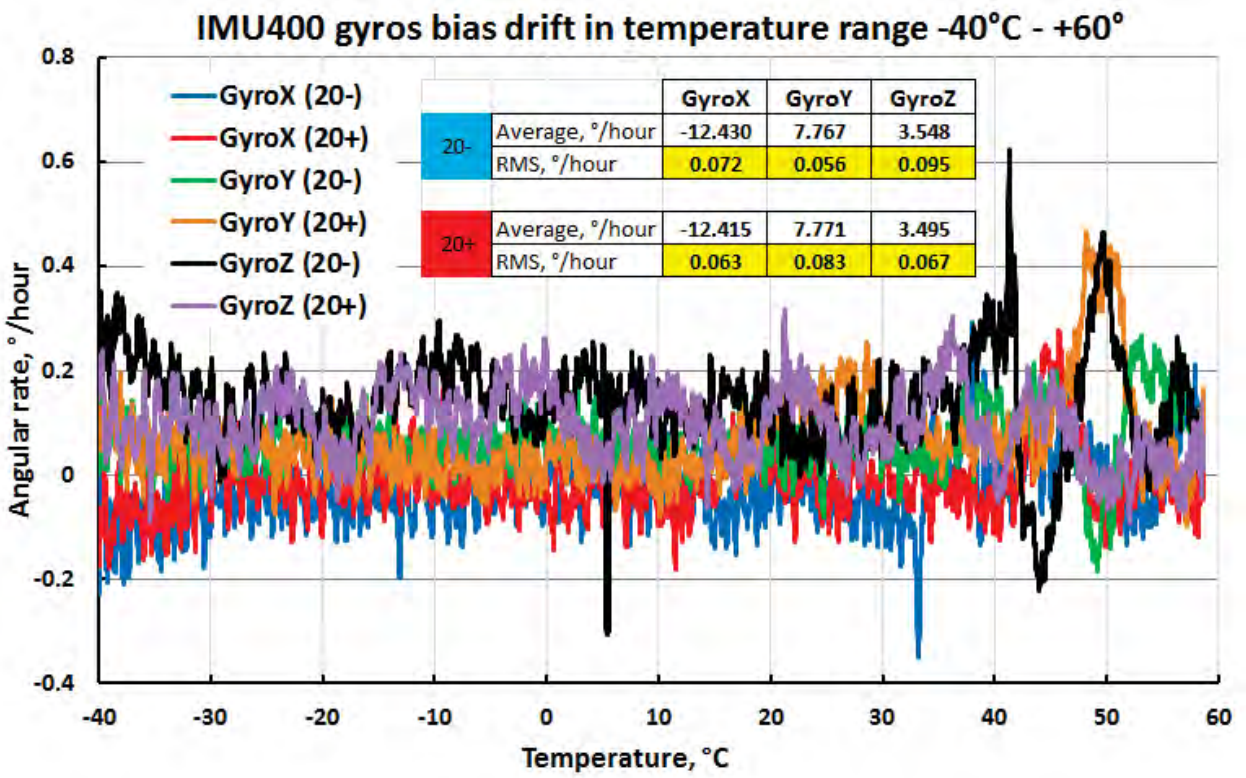

Figure 6. IMU400 Gyroscopes bias stability (drift) plots in temperature range -40°C - +60° with constant temperature change rate ramp +20°C/hour (20+) and -20°C/hour (20-). Absolute values are shifted

For reader's convenience, in order to represent all temperature test data in one plot with single scale of magnitude, Gyro and ACC plots were shifted by constants: -12.4, 7.7, 3.4 °/hour for Gyros X,Y,Z, respectively, and 9.8 m/s^2 for accelerometer X. Real Average/STD data for each channel is presented in captions for each plot in Fig. 4. For ACC X one can see a tail of temperature drift below temperature -33 °C, which is due to the absence of Scale factor calibration settings (points) below this temperature. If needed, it can be compensated further.

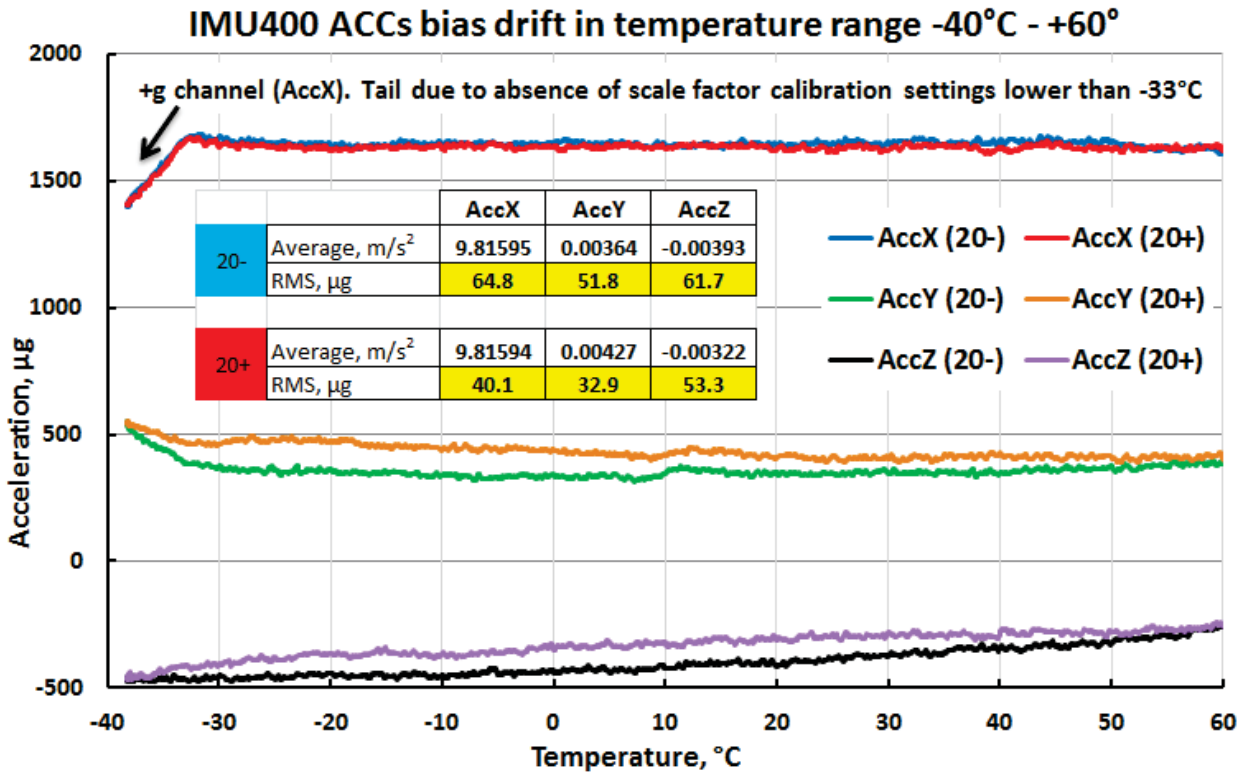

Figure 7. IMU400 ACCs bias stability (drift) plots in temperature range -40°C - +60° with constant temperature change rate ramp +20°C/hour (20+) and -20°C/hour (20-). Absolute values are shifted

All necessary parameters drift in temperature is compensated internally in IMU400 using look-up table (point-like) model with linear interpolation between points. Each parameter has up to 12 compensation points with variable temperature. Temperature-compensated parameters are: gyros bias, gyros scale factor, gyro misalignments, gyro temperature change rate dependence ratios, ACCs bias, ACCs scale factor, ACCs misalignments.

3. IMU400 MEMS-accelerometers testing and IMU schematics improvement

To check the MEMS use feasibility in high dynamic environment, accelerometer scale factor non-linearity tests were performed. Tests included 10 IMU400 devices from 2019-year and 2020–year batches. As long as MEMS ACCs used are 3-axis sensor each, for even and objective estimation the tests were performed in various IMU positions, addressing not only situations of centripetal acceleration directed towards certain IMU axis (Fig. 8a), but also multiple intermediate positions with different angles between centripetal acceleration and IMU sensitivity axes (Fig. 8b). This was done to identify the sensors cross-axis sensitivity in such conditions.

Test setup design included precise rate table (self-made at Optolink) with multiple mounting holes 2 IMU units in tests, balanced with respect to center. Effective radii of IMU rotations was ~10-13cm. Rotation rates were up to 2000°/s.

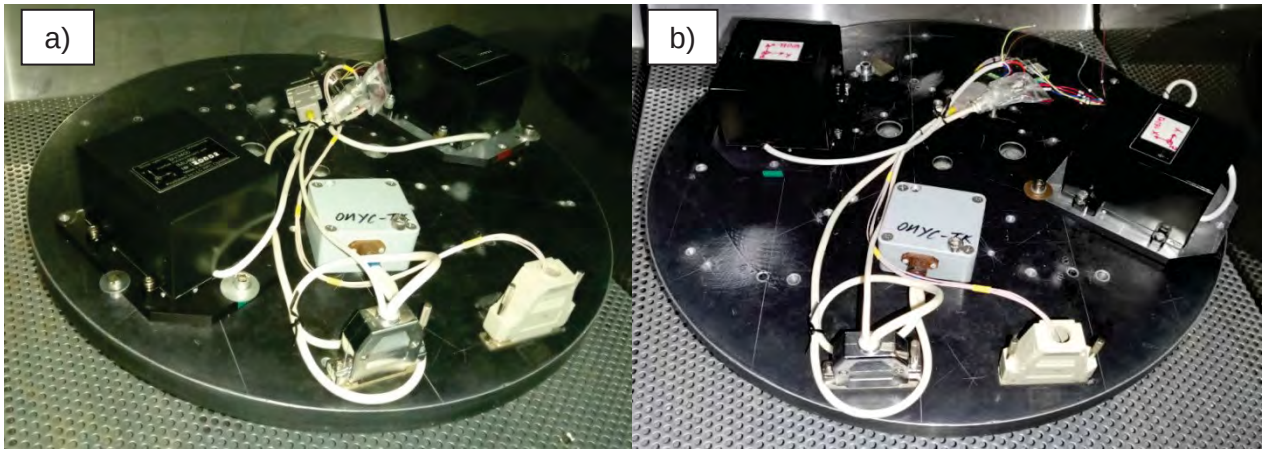

Figure 8. IMU positioning on the rotation table in ACCs scale factor non-linearity tests
a) IMUs with definite axes along centripetal acceleration
b) random acceleration distribution over channels

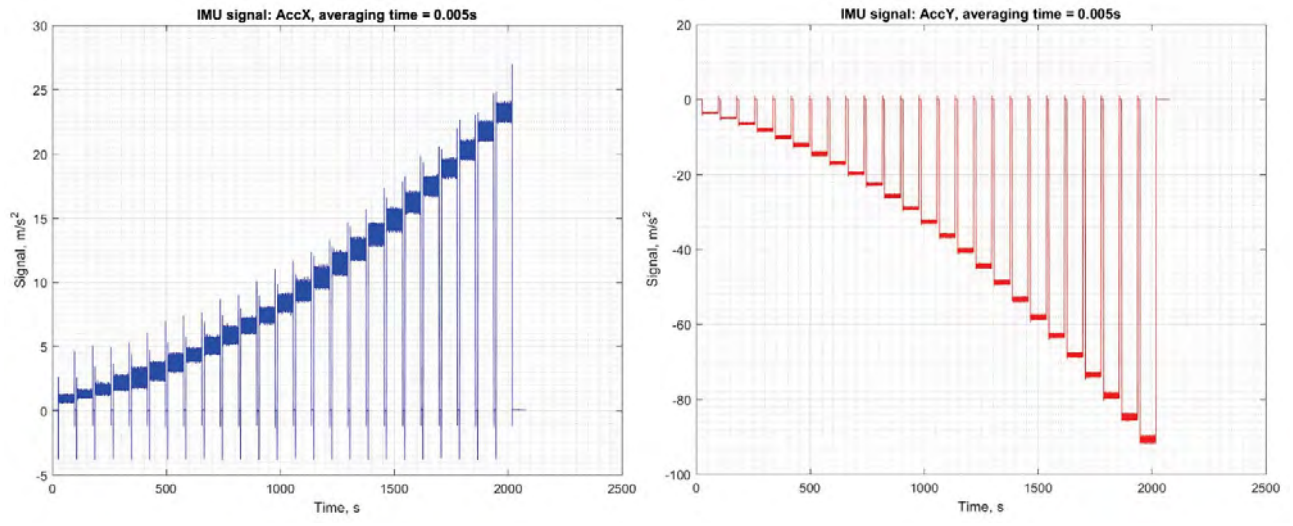

Figure 9. IMU acceleration raw signal for intermediate positions tests (angle ~75°)

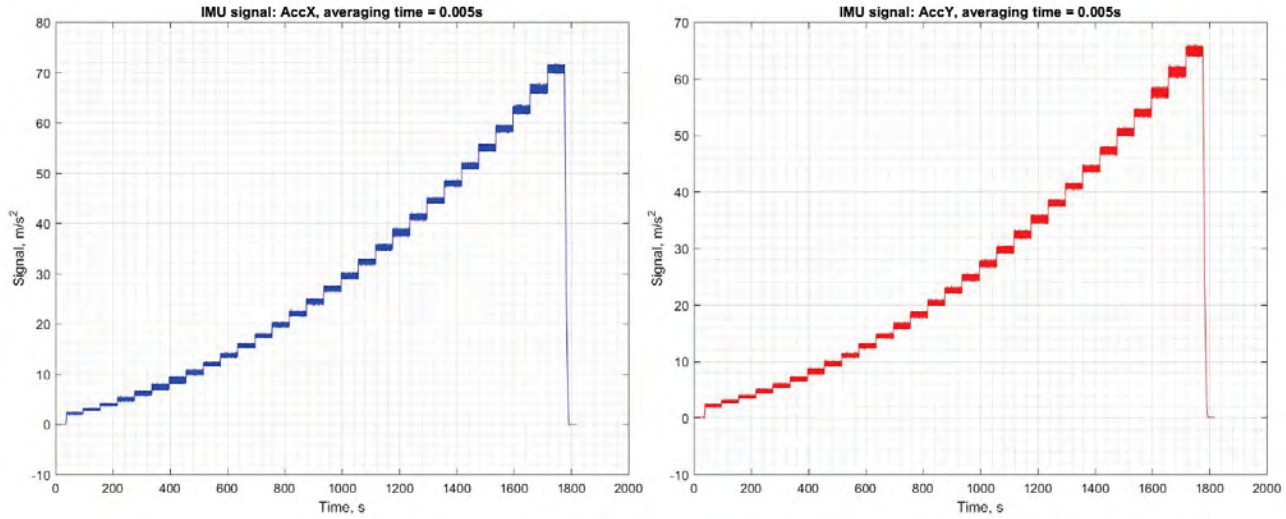

Figure 10. IMU acceleration raw signal for intermediate positions tests (angle ~45°)

Plots of IMU raw signal in some of the test can be found in Fig. 9 and Fig. 10. Several plots of the obtained results for intermediate position tests, as they are most representative ones, are presented in Fig. 11. Obtained results show that accelerometers have predictable non-linearity pattern which can be compensated, if needed. The pattern also tends to have a degree of asymmetricity. Non-linearity errors scale is ~2000ppm at ±10g. However, at ±2g the obtained values are <100ppm. Therefore, for most of IMU general and niche applications like civic, marine, vehicle, there is no need for compensation. This error can be compensated inside IMU, and in general as the values agree for all tested units, corrections can be made preliminarily without direct measuring.

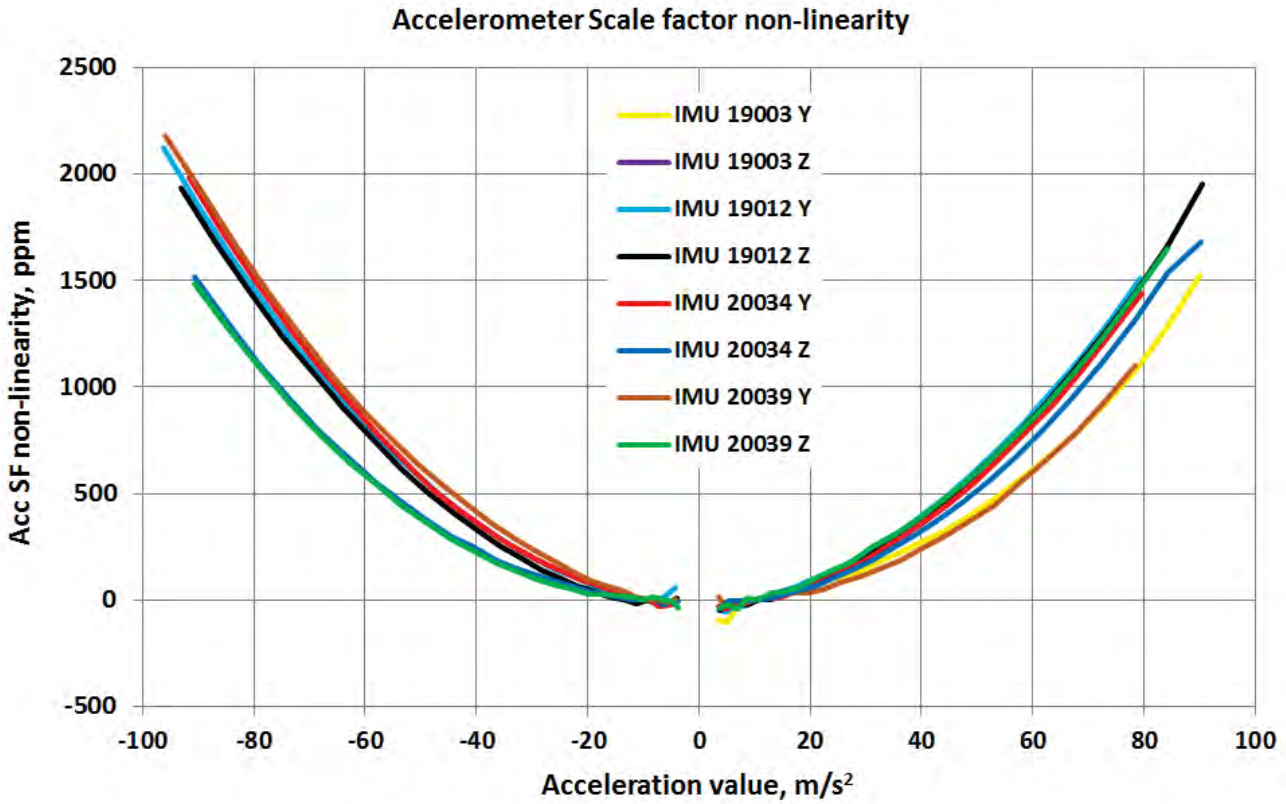

Figure 11. IMU acceleration non-linearity results for intermediate position tests

4. IMU400 schematics improvement: Gyro-Acc time delay

While performing precise inertial calibration of IMU using indirect IMU approach, it was found that during rotations velocities observe sudden shifts. Initial presumption was that this could be associated with accelerometric non-linearity or size effect. But the study of non-linearities showed no peculiarities in ±g range, and due to small arm values its effect could not affect that much, so another reason was searched upon. It was found that if the accelerometer signal during IMU data processing is time-shifted with respect to FOG by certain value, the velocity shifts in rotations disappear (Fig. 12). Then, analyzing IMU schematics for the delay source, we found a peculiarity that gave us frequency-dependent Gyro-Acc delay error – the way the IMU treated Accelerometer signals.

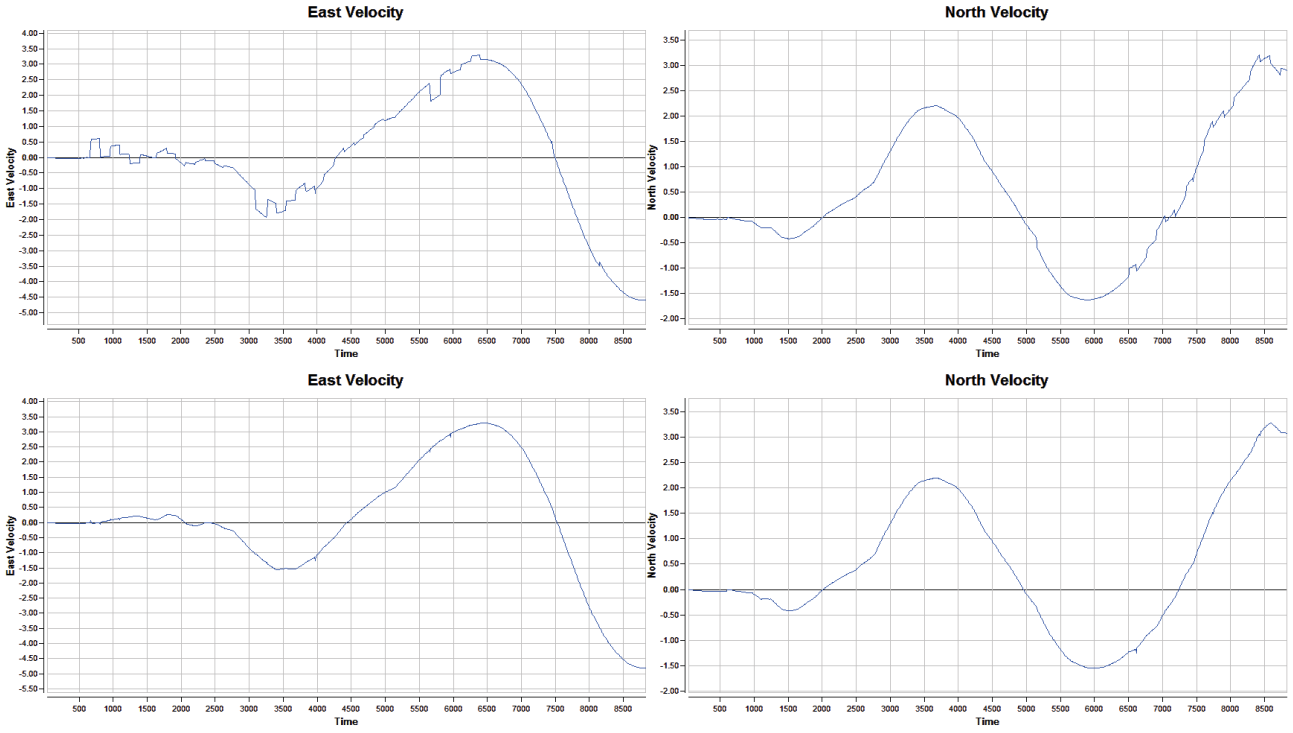

Figure 12. IMU calibration run (simulation). North & East velocity error shifts in rotations (top plots), and this shift is eliminated (bottom plots). Velocities in [m/s]

In special IMU tests aimed to identify the exact delay value, IMU is to be rotated around each gyro axis, but this rotation needs to be around horizontal axis in order for errors to be observable. In simulation tests, with results in Figure 13, IMU400 was rotated 10 times around its each axis, with rotation in vertical plane (around horizontal axis). Gyro-Acc delay was removed in postprocessing (middle image), and then with updated schematics (year 2020) we finally obtain no presence of Gyro-Acc delays (bottom image). For the time being, this delay has been fully eliminated in all supplied IMU400 units.

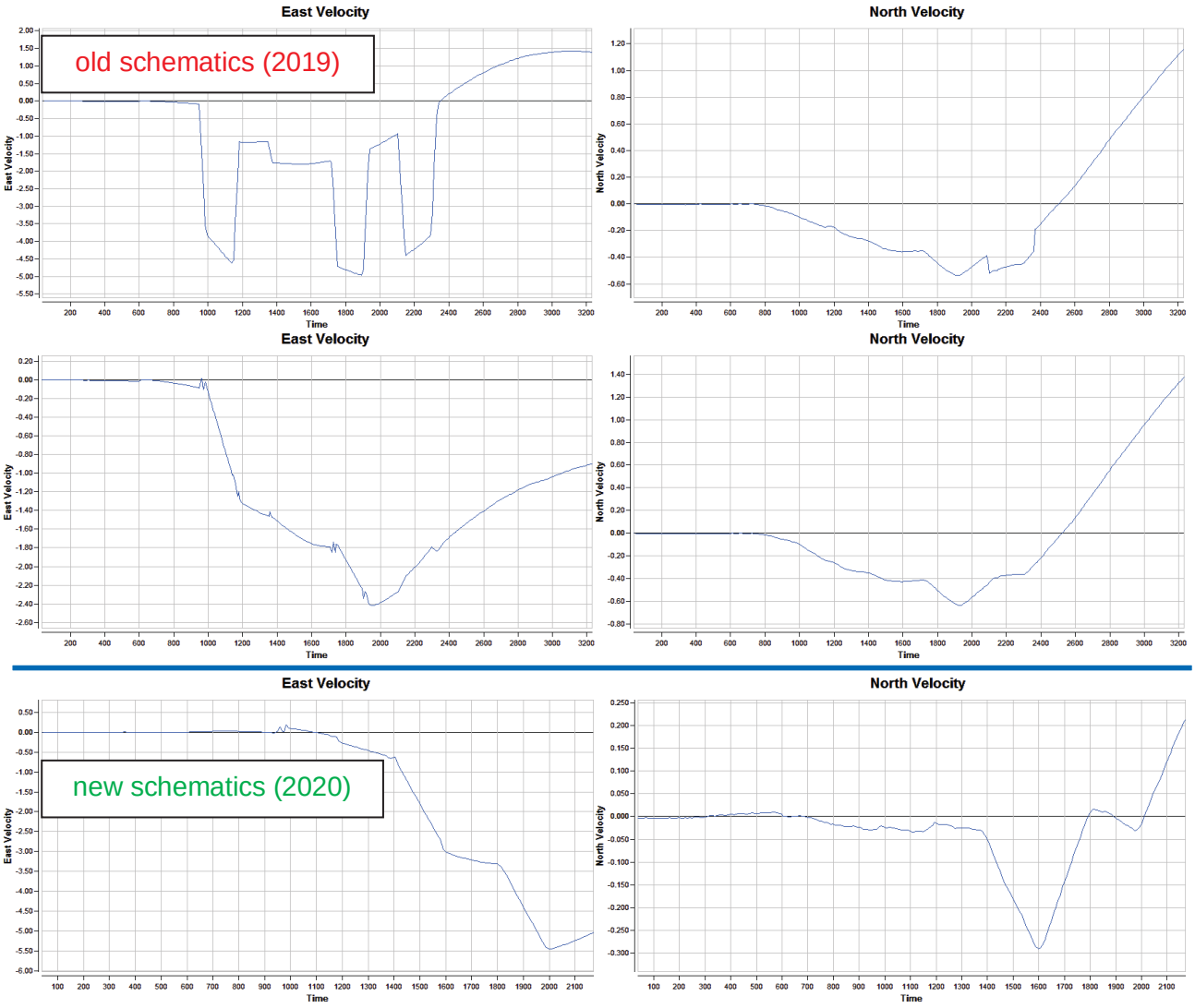

Figure 13. IMU Gyro-Acc time delay run. Top plots – initial schematics test, middle plots – initial schematics test (delay compensated in postprocessing), bottom plots – final IMU schematics test (delay removed inside IMU). Velocities in [m/s]

5. IMU400 simulations testing: gyrocompassing and navigation tests

The performance of IMU400 units after full calibration cycle, temperature dependencies and major biases, was investigated using indirect way of measurements - by SINS modelling software.

At Optolink [8], for SINS certain test procedures are carried out in order to qualify their accuracy level. One of the main and peculiar SINS parameters is the obtained heading accuracy during straightforward alignment in gyrocompassing mode. At Optolink, each SINS runs series of alignment tests, which consist of alignment statistics accumulation over 4 cardinal directions (or more). This test is of importance as it shows not only the noise of sensors (heading RMS with respect to its mean value), but the mean heading errors for each direction, which also represent mainly gyro absolute bias errors and their

stability in time. For example, mean values of obtained heading statistics at directions 0° and 180° allow to identify absolute bias error of sidewinder Gyro of IMU in SINS, as it points East and West in those tests and has thus near-zero angular rate value. And, mean values of heading at directions 90° and 270° allow to identify the absolute bias error of forward Gyro of IMU in SINS. Thus, these tests also can help in precise calibration of gyro biases, and at Optolink these tests are always conducted along with indirect 3-axis rotation table calibration tests (results in Fig. 12) and other stability tests during IMU precise calibration (* additional precise calibration values in Table 1 specifications).

Heading °	1	2	3	4	5	6	Average for	Dispersion for	RMS for Heading, °
0	0.195	0.034	0.380	0.002	0.098	0.279	0.1647	0.0452	**0.212**
90	90.339	90.513	90.541	90.276	90.051	90.398	90.3531	0.1514	**0.389**
180	179.857	179.605	179.770	179.926	179.778	179.731	179.7779	0.0594	**0.244**
270	269.555	269.798	269.531	269.476	269.569	269.804	269.6221	0.1597	**0.400**
0	0.011	-0.192	-0.278	-0.023	0.145	0.115	-0.0226	0.0211	**0.145**

Total disp.	Total RMS
0.0979	**0.313**

	Bias, °/hour		
	X	**Y**	**Z**
test1	0.028	0.054	-0.019
test2	0.036	0.040	0.008

	Cardinal direction					
	0°	90°	180°	270°	0°	**Average**
RMS (Mean-shifted), °	0.147	0.179	0.110	0.142	0.153	**0.146**

Figure 14. IMU400 alignment statistics (10 minutes acquisition time), 4 cardinal directions. Total RMS = 0.313° (Moscow latitude 55.97°). Estimated gyro bias errors are shown. Estimated alignment limit 0.15° ~ 0.1° × sec(lat°) for alignment time 10 minutes.

Alignment tests were carried out with IMU400, alignment statistics accumulated over 4 cardinal directions is presented in Figure 14. Duration of each alignment in statistics is 10 minutes, no overlapping, 4 cardinal directions, 6 alignments per direction. Statistics show heading alignment true error (gyro bias + IMU noise) of 0.3° (at latitude 56°N). Obtained mean heading values at each direction indicate gyro bias errors of: X 0.03°/h, Y 0.05°/h, Z 0.02°/h.

Minimal achievable heading RMS due to only gyro noise level: Estimated alignment limit is 0.146° ~ 0.1°×sec(lat°). Gyro bias changes from test to test comprised at most 0.03°/hour.

Accelerometer biases according to error propagation theory play minor role in the current test, as their influence is an order of magnitude lower than gyros:

- 0.01 °/hour bias error b_ω (small) of gyro pointing East/West corresponds to mean heading error of ~ arctan (b_ω / (15.041×cos(lat°))) = 0.068°; 15.041 °/hour is the value of Earth rotation rate, lat = 55.98° (Moscow).

- 100 μg bias error b_a (moderate) of East ACC corresponds to seeming East gyro deflection by arcsin(b_a/g) = 0.0057° in vertical plane and effectively adds sin(0.0057°)×15.041×sin(lat°) = 0.00125 °/hour to gyro bias bω, resulting into heading error of 0.0085°, according to formula above. Other ACCs biases have almost zero impact.

Alignment-to-alignment stability of Pitch/Roll angles was found to be 0.0017° and 0.0016° (1σ, 10 minutes alignment), respectively, showing performance enough for low-accuracy SINS demands.

After precise accounting for biases, IMU400 at 4 cardinal directions test shows coordinates drift of ~5 Nm over 8 hours in pure inertial mode (no aiding, no Schuler oscillations damping), with 20 minutes alignment (Fig. 15). Schuler velocity amplitude reaches 2 m/s and 4 m/s for East and North velocities.

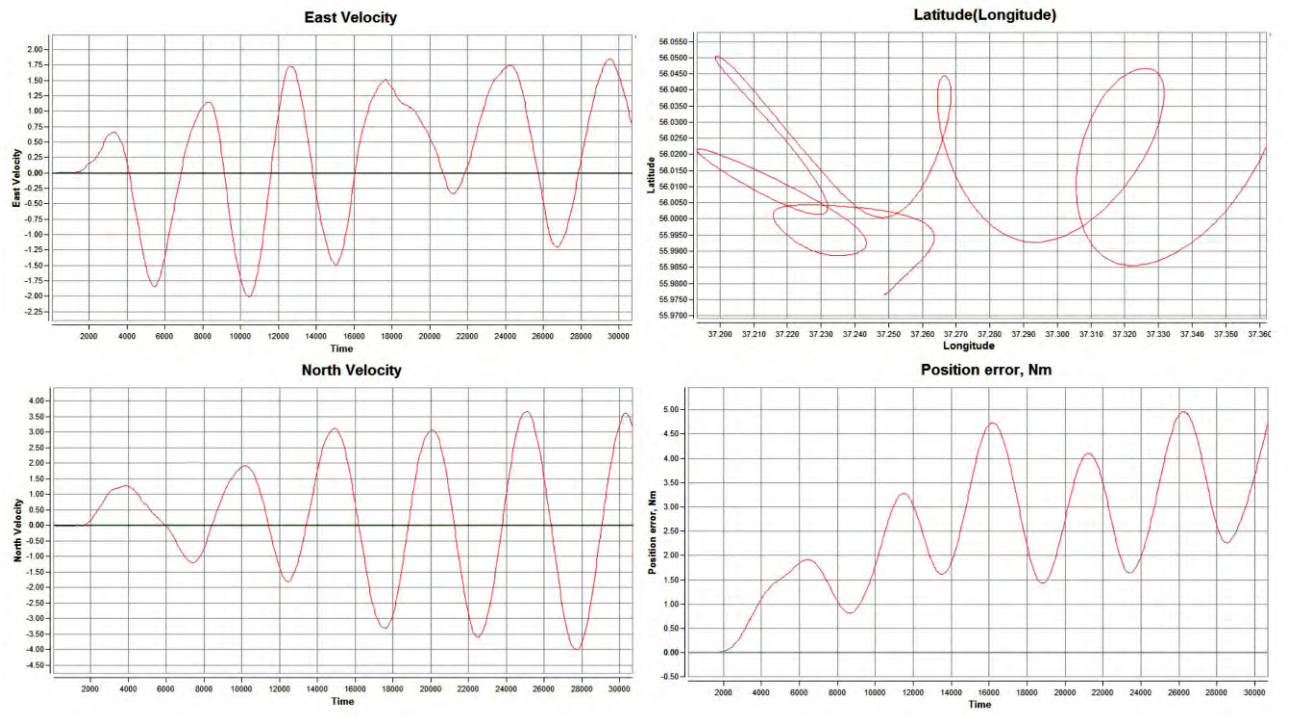

Figure 15. IMU400 navigation performance in pure inertial mode (static), 8 hrs, no aiding, 20 min. alignment, 4 cardinal directions. East & North Velocities in m/s.

Another SINS test is real navigation performance test. In order to perform these tests with IMU not involving SINS equipment, IMU device was being recorded standalone along the track on a vehicle, after that with the SINS simulation software we are able to run the navigation simulation of SINS on the basis of IMU. Each track, IMU data set starts with 10 minutes of static position needed for initial alignment, then the vehicle starts the movement. No aiding data sources are present as IMU is the only data recorded in tests. GPS data for the true track plotting (blue in Figure 7 plots) is available before the IMU tests as the tracks that are used for tests are fixed. GPS data is not synchronized with IMU data thus cannot be used for any kind of IMU aiding or tailoring its path along the way. The only sort of corrections that we used in post-processing was zero velocity update (ZUPT) and Kalman filtration on the basis of velocity errors during ZUPT.

In Fig. 16 and Fig. 17 Navigation performance in two data sets is shown, heading is obtained in true gyrocompassing alignment (10 minutes). First data set is recorded over track of ~30 km (30 minutes of vehicle movement). Second data set is recorded over track of ~110 km (100 minutes of vehicle movement). The presented plots show navigation performance of IMU400 ~1km CPE error and ~10km CPE error, which is several orders of magnitude better than any MEMS or open-loop FOG for the same task (not even measured in pure inertial mode).

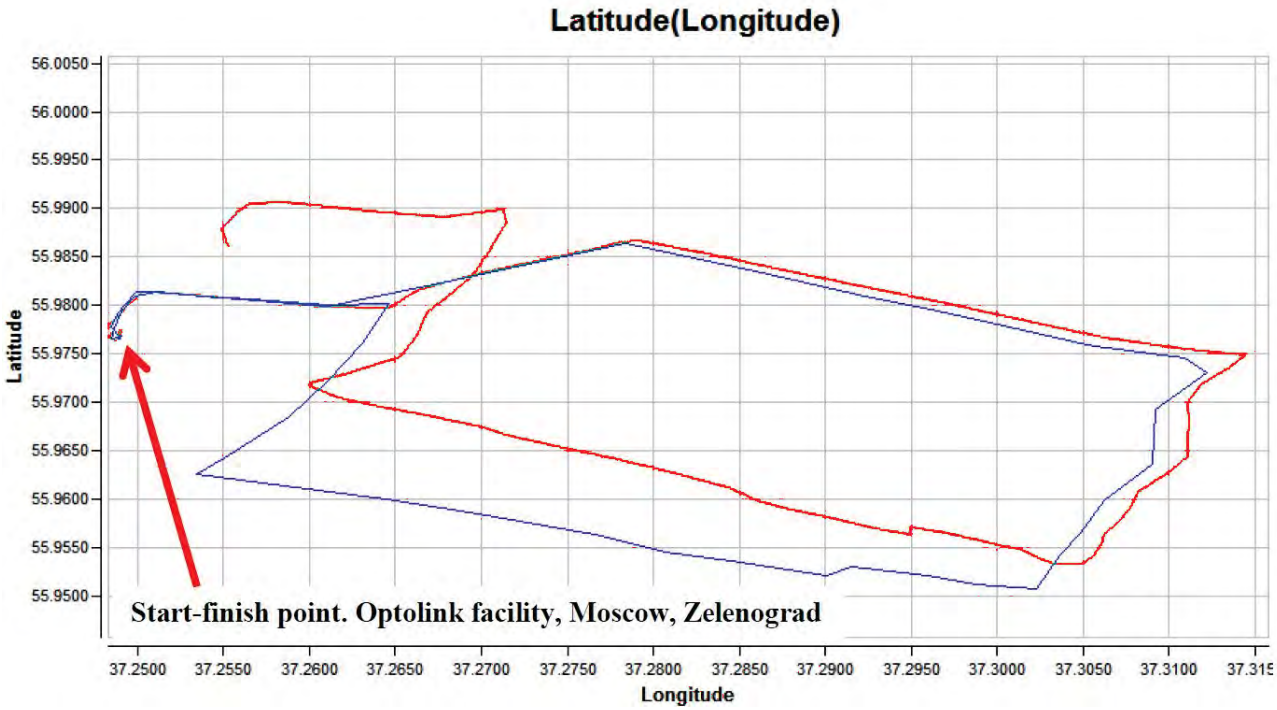

Figure 16. IMU400 navigation performance in inertial mode+ZUPT on track ~20 km, 30 minutes navigation time. CPE error ~1km. Blue is GPS plot, red is IMU postprocessing track

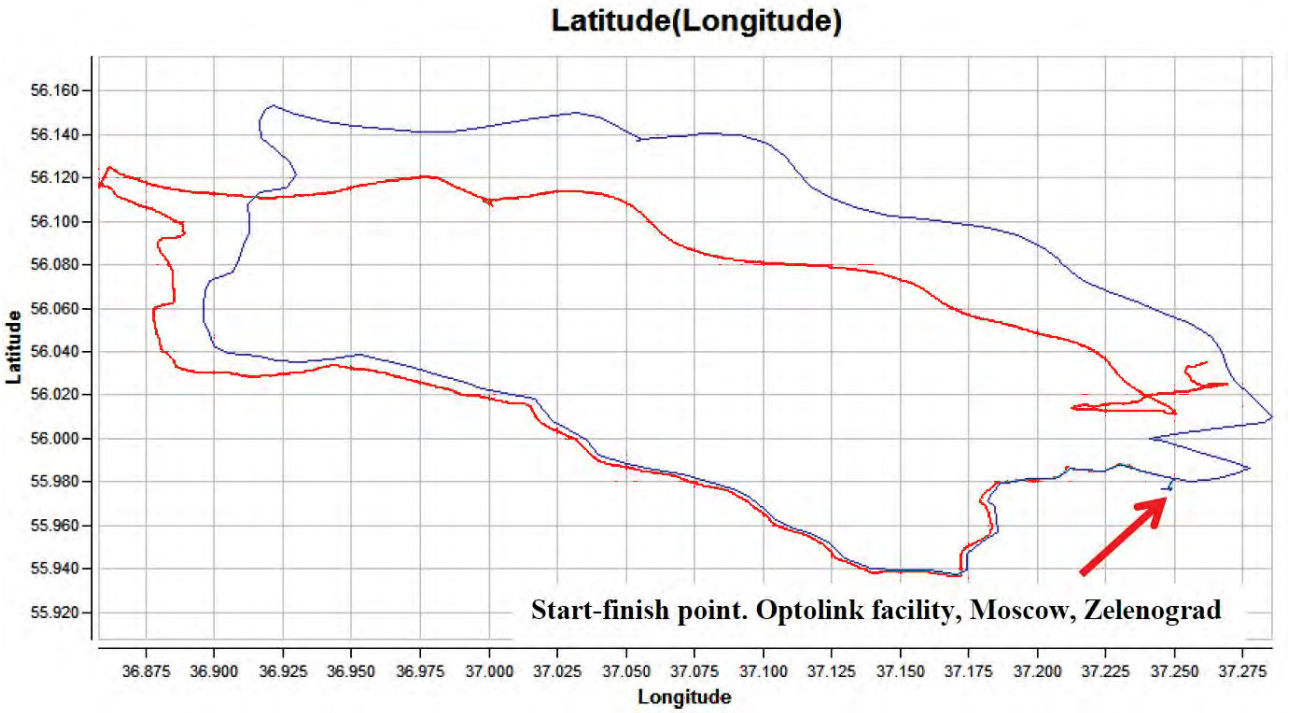

Figure 17. IMU400 navigation performance in inertial mode+ZUPT on track ~110 km, 1.5-2 hours navigation time. CPE error ~10km. Blue is GPS plot, red is IMU postprocessing track

5. Conclusion

In this paper IMU400 characteristics are comprehensively observed: static data (Allan variance), temperature test behavior, accelerometer performance, and SINS simulation results – indirect calibration runs, gyrocompassing accuracy and navigation tests.

The observed performance values allow to assess IMU400 type of devices as navigation or near-navigation grade IMU with unique combination of performance / cost / SWaP characteristics.

References

[1] E. Udd and M. Digonnet, Eds., Design and Development of Fiber Optic Gyroscopes, Bellingham, Washington, SPIE Press, 2019.

[2] F. Guattari, C. Moluçon, A. Bigueur, E. Ducloux, E. de Toldi, J. Honthaas, H. Lefèvre. Touching the limit of FOG angular random walk: Challenges and applications // DGON Intertial Sensors and Systems (ISS) Proceedings, September 20-21, 2016, Karlsrue, Germany, pp.1-13.

[3] Yu.Korkishko, V.Fedorov, V.Prilutskii, V.Ponomarev, I.Morev, S. Kostritskii, A.Zuev, V.Varnakov. Closed loop fiber optical gyroscopes for commercial and space applications // in Proc. Inertial Sensors and Systems - Symposium Gyro Technology 2012, Karlsruhe, Germany, 18-19 September 2012, pp.P14.1-P14.15.

[4] Yu.N.Korkishko, V.A.Fedorov, V.E.Prilutskiy, V.G.Ponomarev, I.V.Fedorov, S.M.Kostritskii, I.V.Morev, D.V.Obuhovich, S.V.Prilutskiy, A.I.Zuev, V.K.Varnakov. Highest bias stability fiber-optic gyroscope SRS-5000 // in Proc. Inertial Sensors and Systems - Symposium Gyro Technology 2017, Karlsruhe, Germany, 19-20 September 2017, pp.P03.1-P03.23.

[5] Yu.Korkishko, V.Fedorov, V.Prilutskii, V.Ponomarev, I.Morev, D. Obuhovich, S.Prilutskii. High-precision fiber optical gyro with extended dynamical range // in Proc. Inertial Sensors and Systems - Symposium Gyro Technology 2014, Karlsruhe, Germany, 16-17 September 2014, pp.P09.1-P09.14.

[6] Yu.N. Korkishko, V.A. Fedorov, V.E. Prilutskiy, V.G. Ponomarev, I.V. Fedorov, S.M. Kostritskii, I.V. Morev, D.V. Obuhovich, S.V. Prilutskiy, A.I. Zuev, V.K. Varnakov. High-precision inertial measurement unit IMU-5000 // in Proc. 2018 IEEE International Symposium on Inertial Sensors and Systems, pp.111-114.

[7] Yu.N. Korkishko, V.A. Fedorov, V.E. Prilutskiy, V.G. Ponomarev, I.V. Morev, A.I. Morev, D.V. Obuhovich, S.M. Kostritskii, A.I. Zuev, V.K. Varnakov, A.V. Belashenko, E.N. Yakimov, G.V. Titov, A.V. Ovchinnikov, I.B. Abdul'minov, S.V.Latyntsev. Space grade fiber optic gyroscope: R&D results and flight tests // in Proc. 2016 DGON Inertial Sensors and Systems (ISS), Karlsruhe, Germany, 20-21 September 2016, pp.21.1-21.19.

[8] Yu.N.Korkishko, V.A.Fedorov, V.E.Prilutskii, V.G.Ponomarev, I.V.Morev, S.F.Skripnikov, M.I.Khmelevskaya, A.S.Buravlev, S.M.Kostritskii, I.V.Fedorov, A.I.Zuev, V.K.Varnakov. Strapdown Inertial Navigation Systems Based on Fiber Optic Gyroscopes // Gyroscopy and Navigation, 2014, Vol. 4, No. 4, pp. 195–204.